Sensitivity of CyGNSS to Above Ground Biomass and Canopy Height over Tropical Forests

H. Carreno-Luengo,* G. Luzi, and M. Crosetto

Centre Tecnòlogic de Telecomunicacions de Catalunya (CTTC/CERCA), Castelldefels (Barcelona), Spain
Tel. +34 93 645 29 00
*Corresponding author: hugo.carreno@cttc.cat

An experimental assessment of the performance of Global Navigation Satellite Systems Reflectometry (GNSS-R) for biomass monitoring over tropical forests is presented. Several observables of the so-called Delay Doppler Maps (DDMs), as provided by the Cyclone Global Navigation Satellite Systems (CyGNSS) microsatellites constellation, are evaluated using the pan-tropical Above Ground Biomass (AGB) map provided by Avitabile et al. and Canopy Height (CH) data derived from the Geoscience Laser Altimeter System (GLAS) lidar-instrument on-board the National Aeronautics and Space Administration NASA's Ice, Cloud, and land Elevation Satellite (ICESat). In so doing, different tropical forests types are studied. Preliminary results show that the spreading of the DDMs in the delay domain has a sensitivity up to a mean AGB ~ 325 ton/ha over Congo rainforests for elevation angles in the range θ_e ~ [20, 40] º.

Index Terms— GNSS-R, CyGNSS, Above Ground Biomass (AGB), canopy height, tropical forests, coherent and incoherent scattering

1. Introduction

Quantifying the global carbon cycle is essential to understand many of the dramatic changes taking place in the Earth's system, particularly those resulting from the burning of fossil fuel and land-use change. Forests absorb, store, and release large amount of carbon. Therefore, they are a key component of the carbon cycle. The sensitivity to biomass of current space-borne L-band radar saturates at ~ 150 ton/ha. The future European Space Agency ESA's BIOMASS mission is aimed to overcome this limitation using P-band and a 12-m deployable reflector antenna. The potential use of GNSS-R for biomass monitoring has been previously studied in several theoretical and experimental works [1,2]. In this work, the performance of CyGNSS for biomass monitoring is evaluated over tropical forests.

2. Forests Biomass Studies with GNSS-R: Theoretical Considerations

Classical monostatic radar missions measure the radar backscatter, which typically saturates for relatively low levels of biomass. On the other hand, the intrinsic bistatic geometry of GNSS-R enables to collect both the coherent and the incoherent components of the total scattered electromagnetic field. As such, the bistatic scattering coefficient σ^0 is defined as follows:

$$\sigma^0 = \sigma^{incoh,0} + \sigma^{coh,0}, \quad (1)$$

where $\sigma^{incoh,0}$ and $\sigma^{coh,0}$ are the incoherent and the coherent terms respectively.

L-band GNSS signals can partially penetrate the vegetation cover because of the improved signal penetration depth as compared to higher frequency bands. The total reflected power collected by a GNSS reflectometer is composed of several contributions: (a) direct scattering over the soil surface, (b) direct scattering over the vegetation cover (leaves, branches, and trunks), and (c) multiple scattering that involves the soil surface and the vegetation cover. The polarization of the GNSS signals changes from Right Hand Circular Polarization (RHCP) to Left-HCP after direct scattering. On the other hand, they become RHCP after multiple scattering (first from RHCP to LHCP, and then from LHCP to RHCP). The contributions to the incoherent scattering term $\sigma^{incoh,0}$ are surface scattering over the soil due to roughness effects, and volume scattering over the vegetation cover. On the other hand, the coherent scattering term $\sigma^{coh,0}$ is mainly associated to the soil surface. Coherence effects could also appear after scattering over the vegetation cover if the coherent integration time T_c is set to be long enough e.g. ~ 20 ms, so as to filter out the noise and the volume scattering term. However, the volume scattering term is significant for lower integration times ~ 1 ms (e.g. CyGNSS).

The signals that are coherently scattered over the surface suffer attenuation and depolarization along the direct and reflected paths because of the effects of scattering and absorption by the vegetation cover. These effects are stronger over areas with high levels of vegetation. However, the coherent reflected power is roughly independent of the platform's height in a Low Earth Orbit (LEO) scenario as:

$$\left\langle \left|Y_{r,coh}(\tau,f)\right|^2 \right\rangle = \frac{P_T \lambda^2 G_T G_R \left|\chi(\tau,f)\right|^2}{(4\pi)^2 (R_T + R_R)^2} \left|R_p(\theta_e)\right|^2 \exp(-2k\sigma \sin\theta_e)^2, \quad (2)$$

where P_T is the transmitted power, G_T and G_R are the gain of the transmitting and receiving antennas, R_T and R_R are the ranges from the transmitter and the receiver to the specular point, respectively, χ is the Woodward Ambiguity Function (WAF), τ is the delay of the signal from the transmitter to the receiver, f is the Doppler shift of the electromagnetic reflected signal, R_p is the p-polarized Fresnel reflection coefficient, k is the signal angular wavenumber, and σ is the surface height standard deviation (related to surface roughness). On the other hand, the incoherently scattered signals suffer stronger free space losses. Consequently, $\left\langle \left|Y_{r,coh}(\tau,f)\right|^2 \right\rangle$ could overpass the incoherent term $\left\langle \left|Y_{r,incoh}(\tau,f)\right|^2 \right\rangle$ even from a spaceborne platform. Finally, it is worth to point out that the effects of soil variables such as Soil Moisture Content (SMC) and surface roughness in the DDMs $\left\langle \left|Y_r(\tau,f)\right|^2 \right\rangle$ are lower than the effects of forests biomass for high levels of vegetation [1].

3. Methodology

3.1 Definition of the Selected CyGNSS Observables

CyGNSS Level 2.1 Science Data Record [3] is selected for this study. Reflected delay waveforms $WF_{r,raw}$ are obtained from the original DDMs $\left\langle \left|Y_r(\tau,f)\right|^2 \right\rangle$ at zero Doppler frequency:

$$WF_{r,raw} = \left\langle \left|Y_r(\tau, f=0)\right|^2 \right\rangle. \quad (3)$$

The delay bin resolution of the original 17-lag waveforms $WF_{r,raw}$ is ~ 0.2552 GPS C/A chips. An optimum re-sampling and interpolation of the resulting 1700-lag waveforms is performed using a spline method to increase the accuracy of the waveforms, before applying the algorithms to extract the observables. Several observables are considered to evaluate the sensitivity of $\sigma^{coh,0}$ and the volume scattering term to forests biomass.

The width of the trailing edge (TE) is defined as the lag difference between a certain power threshold of the high-resolution waveforms $WF_{r,threshold}$ and the corresponding to the maximum power of the waveforms $WF_{r,peak}$:

$$TE = \tau_{WF_{r,threshold}} - \tau_{WF_{r,peak}}. \quad (4)$$

The incoherent scattering term $\sigma^{incoh,0}$ is the main contribution to $WF_{r,threshold}$, while both the coherent $\sigma^{coh,0}$ and the incoherent $\sigma^{incoh,0}$ scattering terms significantly contribute to the peak power of the waveforms $WF_{r,peak}$. The width of the leading edge (LE) is defined using a similar approach.

The ratio R of the trailing TE over the leading LE edges width is further evaluated as a complementary observable. It is defined as follows:

$$R = TE / LE. \quad (5)$$

R equals 1 for a complete flat surface, as an indication that the GNSS signals are reflected in a specular manner. On the other hand, it increases as larger is the surface roughness σ because the number of surface facets that contributes to $\left\langle \left|Y_r(\tau,f)\right|^2 \right\rangle$ becomes higher. However, its performance for biomass monitoring remains unexplored.

The reflectivity Γ_{rl} is estimated as the ratio of the reflected $WF_{r,peak}$ and the direct $WF_{d,peak}$ power waveforms peaks, after compensating for the noise power floor and the antennas' gain patterns as a function of the elevation angle θ_e:

$$\Gamma_{rl} = WF_{r,peak} / WF_{d,peak}, \quad (6)$$

where the subscript rl denotes the incident (r, RHCP) and the scattered polarization (l, LHCP).

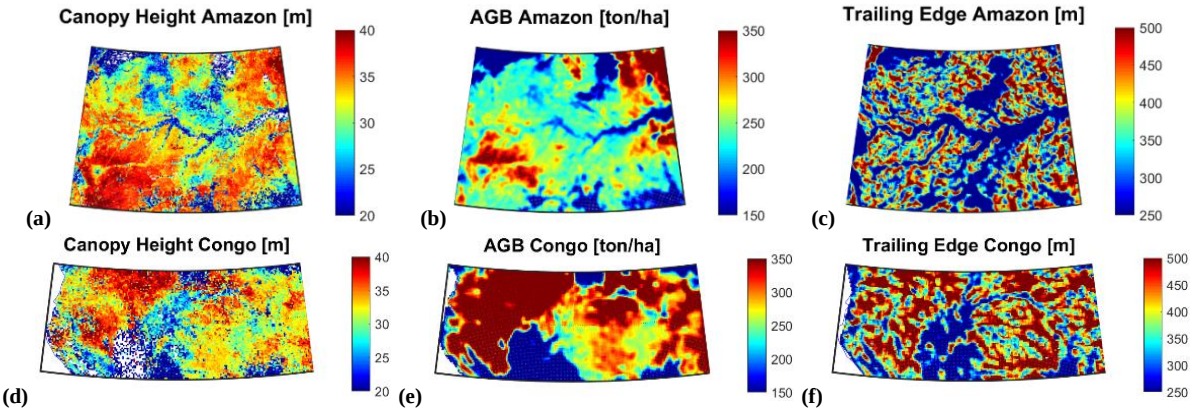

Fig. 1. Biomass study over Amazon ((a) Canopy height (CH), (b) Above Ground Biomass (AGB), (c) CyGNSS 70% trailing edge (TE) width) and Congo ((d) CH, (e) AGB, (f) CyGNSS 70% TE width) tropical rainforests.
Amazon: Lat. = [-11, 5] º, Lon. = [-75, -54] º. Congo: Lat. = [-4, 4] º, Lon. = [9, 28] º.

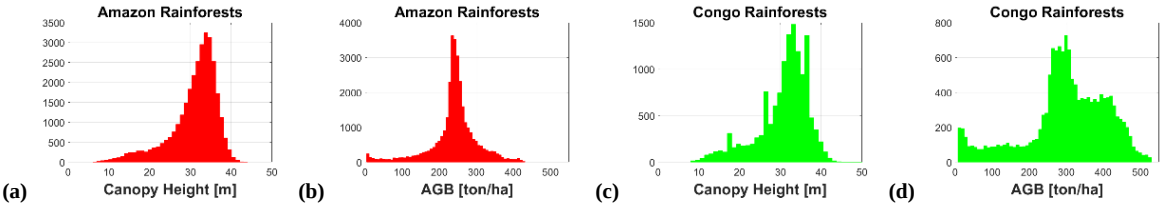

Fig. 2. Histograms over Amazon ((a) Canopy Height (CH), (b) Above Ground Biomass (AGB)) and Congo ((c) CH, (d) AGB).

3.2 Strategy

DDMs are classified into different groups according to different ranges of the satellites' elevation angle $\theta_e \sim [70, 90]$ º, $\theta_e \sim [45, 65]$ º, and $\theta_e \sim [20, 40]$ º because θ_e is an important parameter that determines the ratio of the coherent $\left\langle \left| Y_{r,coh}(\tau,f) \right|^2 \right\rangle$ to incoherent $\left\langle \left| Y_{r,incoh}(\tau,f) \right|^2 \right\rangle$ scattering components. Additionally, several TE thresholds are evaluated that correspond to 50% ($WF_{r,0.5}$), 70% ($WF_{r,0.7}$), and 90% ($WF_{r,0.9}$) of the maximum power of the waveforms $WF_{r,peak}$. The soil surface contribution to the incoherent scattering term $\sigma^{incoh,0}$ is filtered out to evaluate only the effect of the volume scattering term. In so doing, only pixels over the surface with a Terrain Ruggedness Index (TRI) lower than 5 are considered [4]. This threshold was found empirically to limit significantly the effect of the topography in $\left\langle \left| Y_r(\tau,f) \right|^2 \right\rangle$. The observables are averaged using a 0.1 º x 0.1 º latitude/longitude grid with a moving window of 0.2 º, within a temporal window of 1-month (18/03/2018 to 18/04/018). This strategy enables the analysis using auxiliary data from different sensors with a different spatial resolution.

4. Canopy Height and Above Ground Biomass Reference Data

Tropical rainforests [Fig. 1] are hot ecosystems with wet biomass where it rains along the year, leading to small temporal fluctuations of SMC. They are characterized by high and dense canopies of vegetation that form different layers, being the vegetation organized following a vertical pattern from the soil to the canopy. The global canopy height [Figs. 1a,d and Figs. 2a,c] map produced by the GLAS lidar-instrument on-board ICESat is used as the canopy height reference (2004-2008) [5]. This map incorporates auxiliary data from the Moderate Resolution Imaging Spectroradiometer (MODIS) and the Tropical Rainfall Measuring Mission (TRMM) to generate the final product. The applied algorithm [5] uses a height correction factor based on the trailing waveform edge extent to correct for topographic effects because of the non-homogeneous sampling properties of GLAS. The original spatial resolution of this map is ~ 0.2 km. The integrated pan-tropical map by Avitabile et al. [6] is selected as the AGB reference [Figs. 1b,e and Figs. 2b,d]. It should be understood as aboveground live woody biomass. This map combines two different AGB datasets into a ~ 1 km resolution product. In so doing, it uses an independent reference of field observations for validation and highly resolution biomass maps locally-calibrated, harmonized, and upscaled to 14,477 ~ 1 km AGB estimates as inputs for the fusion algorithm. This data fusion approach applies bias removal and weighted linear averaging. It uses and spatializes the AGB patterns of the reference datasets of Saatchi and Baccini [6], which have significant differences. Both patterns use the same primary data source (GLAS), similar strategy to upscale lidar-data, and they assume continental allometric relationships.

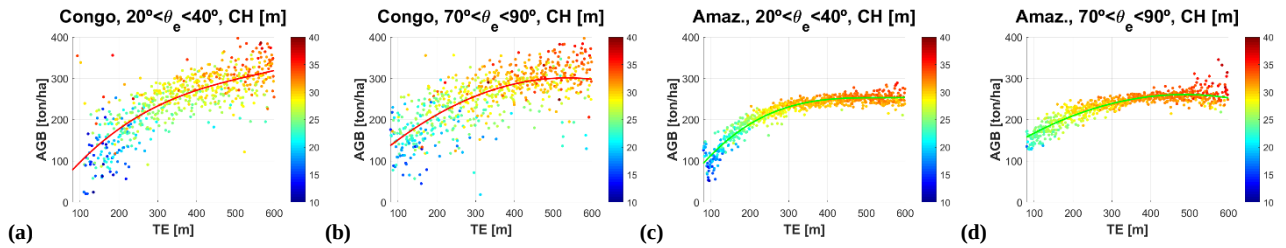

Fig. 3. Relationships between the 70% TE width and AGB over (a), (b) Congo and (c), (d) Amazon tropical rainforests for different ranges of the elevation angle (a), (c) θ_e ~ [20, 40] º, and (b), (d) θ_e ~ [70, 90] º, as a function of the Canopy Height (CH).

5. Preliminary Results: Evaluation of the 70% Trailing Edge Width vs. AGB over Tropical Rainforests

The scatter plots between the 70% TE width and the AGB over Congo and Amazon rainforests are computed using the mean values of both observables in steps of TE ~ 1 m [Fig. 3]. This strategy allows to reduce noise at pixel level, such as speckle in $Y_r(\tau, f)$ and potential errors in GLAS-derived AGB. The extension of the target areas is large, providing enough data. The errors are assumed to be randomly distributed. Thus, the noise can be reduced after averaging, so as to find the underlying correlation between both observables. This functional correlation is fitted by an empirical quadratic polynomial function over Congo [Figs. 3a,b] and Amazon [Figs. 3c,d] at different angular ranges θ_e ~ [20, 40] º [Figs. 3a,c] and θ_e ~ [70, 90] º [Figs. 3b,d]. Preliminary results show that TE is more spread with increasing AGB levels up to ~ 325 ton/ha at θ_e ~ [20, 40] º vs. ~ 300 ton/ha at θ_e ~ [70, 90] º over the Congo, and up to ~ 250 ton/ha over the Amazon at both angular ranges. TE increases as larger is the amount of biomass because: (a) The higher volume scattering term in $\sigma^{incoh,0}$ increases the tail of $\left\langle |Y_r(\tau,f)|^2 \right\rangle$. (b) The coherent scattering term $\sigma^{coh,0}$ is more attenuated for increasing vegetation levels. On the other hand, the TE shows a higher sensitivity to AGB as lower is θ_e down to ~ 90 ton/ha at θ_e ~ [20,40]º vs. ~ 140 ton/ha at θ_e ~ [70,90]º over Congo, and ~ 100 ton/ha at θ_e ~ [20,40]º vs. ~ 160 ton/ha at θ_e ~ [70,90]º over the Amazon. The improved sensitivity at lower angles could be explained because of the higher coherent reflectivity for lower angles (eqn. 2). This characteristic increases the dynamic range of the Signal-to-Noise Ratio (SNR), which in turn belongs to a higher sensitivity to the upwelling attenuating cover.

6. Conclusions and Final Discussions

Earth-reflected L1 GPS signals as collected in a bistatic radar configuration by the CyGNSS constellation using down-looking LHCP antennas with relatively low gain ~ 15 dB show an improved sensitivity at θ_e ~ [20, 40] º as compared to θ_e ~ [70, 90] º, up to AGB ~ 325 ton/ha over Congo rainforests, and without an apparent signal saturation level. Overall, the higher sensitivity over the Congo is justified because the dynamic range of the AGB ~ [0, 550] ton/ha is higher than that over Amazon rainforests. The sensitivity over Congo rainforests shows a higher variability with θ_e than over the Amazon, at high levels of AGB. This observation could be linked to different structural properties of the vegetation cover. The AGB distribution over the Amazon seems to be roughly like a Gaussian one and the re-radiation pattern could have isotropic properties. This characteristic explains the small angular variability of the sensitivity. On the other hand, a bimodal distribution is found over the Congo, belonging to a much more complex structure of the canopy layer and a higher angular variability of the sensitivity. A wide variety of tropical regions including moist-, dry-, and coniferous forests is also under study.

7. References

[1] P. Ferrazzoli, L. Guerriero, N. Pierdicca, and R. Rahmoune, "Forest biomass monitoring with GNSS-R: theoretical simulations," Elsevier, Adv. Space Res., vol. 47, no. 10, pp. 1823-1832, May 2011. [Online]. Available https://doi.org/10.1016/j.asr.2010.04.025 (accessed on 11/01/2019) [2] M. Zribi, D. Guyon, E. Motte, S. Dayau, J.-P. Wigneron, N. Baghdadi, and N. Pierdicca, "Performance of GNSS-R GLORI data for biomass estimation over the Landes forest," Elsevier, Int. J. Appl. Earth Obs. Geoinformation, vol. 74, pp. 150-158, Feb. 2019. [Online]. Available https://doi.org/10.1016/j.jag.2018.09.010 (accessed on 15/01/2019) [3] CYGNSS. 2017. CYGNSS Level 1 Science Data Record. Ver. 2.1. PO.DAAC, CA, USA. [Online]. Available http://dx.doi.org/10.5067/CYGNS-L1X20 (accessed on 11/11/2018) [4] G. Amatulli, S. Domisch, M.-N. Tuanmu, B. Parmentire, A. Ranipeta, J. Malczyk, and W. Jetz, "A suite of global cross-scale topographic variables for environmental and biodiversity modelling," Nature Scientific data, Mar. 2018. DOI: 10.1038/sdata.2018.40 [5] S.P. Healey, M.W. Hernandez, D.P. Edwards, M.A. Lefsky, E. Freeman, P.L. Patterson, E.J. Lindquist, and A.J. Lister. 2015. CMS: GLAS LiDAR-derived Global Estimates of Forest Canopy Height, 2004-2008. ORNL DAAC, Oak Ridge, Tennessee, USA. [Online]. Available http://dx.doi.org/10.3334/ORNLDAAC/1271 (accessed on 8/11/2018) [6] V. Avitabile et al., "An integrated pan-tropical biomass map using multiple reference datasets," John Wiley and Sons Ltd., Global Change Biology, vol. 2, no.4, pp. 1406-1420. Apr. 2016. [Online]. Available https://doi.org/10.1111/gcb.13139 (accessed on 2/11/2018)

Acknowledgements: This research was carried out with the support grant of a Juan de la Cierva research fellowship from the Spanish Ministerio de Economia, Industria y Competitividad (MINECO), reference FJCI-2016-29356.